

Volume reflection in a bent crystal with purely parabolic inter-planar potentials

M. V. Bondarenko

Kharkiv Institute of Physics and Technology, 1 Academichna St., 61108 Kharkiv, Ukraine.

(Dated: December 1, 2021)

For trajectory of a particle undergoing volume reflection in a bent crystal an explicit expression is obtained, within the model of parabolic continuous potential in each inter-planar interval, and with the neglect of multiple scattering. For the case of bending radius well exceeding the critical value, a formula is derived for the final volume reflection angle in units of Lindhard's critical angle, and for the acquired beam angular spread.

PACS numbers:

Keywords: scattering in a central potential; volume reflection

I. INTRODUCTION

Volume reflection [1, 2] is the effect of beam deflection upon high-energy charged particle over-barrier passage through a bent crystal with bending radius R larger than the critical value R_c . Characteristically, the deflection occurs to the side opposite to that of the crystal bending, and the value of the deflection angle, as inferred from numerical simulations, is of the order of the critical angle for the given energy, but somewhat different for positive and negative particles, whereas the angular dispersion is much less than the mean deflection. There are suggestions to utilize this effect for beam partial extraction at large accelerators [?].

From the theoretical point of view, the problem reduces to a 1-dimensional one in radial coordinates [1], but still is not completely trivial. The precise limiting ratio of the mean deflection angle to the critical is unknown, let alone the acquired angular width (the numerical study of those observables was given in [3] based on a precise Si (110) inter-planar continuous potential). Ultimately, one wishes to know an analytic expression for the particle trajectory, which might serve as a basis for evaluation of the emitted electromagnetic radiation, etc. Realizing the complexity of the integration problem, and of the limiting procedures involved (large crystal thickness, and $R \approx R_c$), in the present paper we scrutinize the simplest model of parabolic continuous potential between the atomic planes, neglecting the multiple scattering on individual nuclei.

The parabolic potential in each separate inter-planar interval actually represents a harmonic oscillator, which admits simple analytic evaluation of the trajectory. It remains to connect the solutions on the boundaries of the adjacent intervals (however, this must be done transitively, for an arbitrarily large number of intervals, e. g., with the use of mathematical induction. Thereupon, one needs to express the final deflection angle, analyze its limiting behavior at $R \approx R_c$, etc. There are also expected some differences in the motion of positively and negatively

charged particles. We start considering those two cases in parallel, but when coming to evaluation of the volume reflection angle, they need separate treatment.

In Sec. II we implement the procedure of solution connection from interval to interval by mathematical induction, and express the particle trajectory as an explicit function of the interval order number. In Sec. III we find the reflection point and evaluate the reflection angle for an arbitrary ratio R/R_c . In Sec. IV we scrutinize the limit $R \approx R_c$, most interesting from the viewpoint of volume reflection, first for positively, then for negatively charged particles. We evaluate the differential cross-section as a function of the reflection angle variation. In Sec. V we comment on the opposite limit $R \gg R_c$. A summary is given in Sec. VI.

II. PARTICLE TRAJECTORY IN THE BULK OF THE CRYSTAL

A. Initial conditions

To establish connection of the passing particle coordinates with the impact parameters, and to start the mathematical induction procedure, let us begin with the description of particle passage through the first hit inter-planar interval. Let z -axis be directed precisely along the particle incidence direction, x -axis be perpendicular to it in the plane of crystal bending. Choose the coordinate origin at the front face, in the middle of the interval which the particle hits first. Let $\theta_0 > 0$ be the (small) angle of inclination of crystalline planes at the front face (see Fig. 1). The precise angle of the crystal front face inclination to the x axis is of little consequence, if the particle penetrates deeply into the crystal; we shall assume that the front face is defined by the condition $z = 0$. Upon the entrance of the fast charged particle to the crystal, one may treat the interaction with the inter-crystalline fields as mere influence of an averaged along planes, so-called continuous, potential, creating a transverse force. The longitudinal component of the force, as well as the edge effects at the entrance to the crystal may certainly be neglected for an ultra-relativistic particle.

In monocrystals of not too heavy chemical elements,

Electronic address: bon@kipt.kharkov.ua

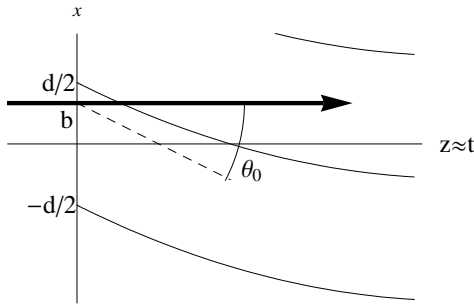


FIG. 1: Particle variables at the entrance to the bent crystal.

in particular for silicon, in orientation (110) [8] the interplanar potential may with a fair accuracy be approximated by a parabola. That implies the differential equation of motion of the classical ultra-relativistic particle to be

$$x = \frac{2F_{max}}{Ed} (x + x_0); \quad (1)$$

where E is the particle energy, d is the interplanar distance, F_{max} is the force acting on a positively charged particle at the edge of the interplanar interval $x - x_0 = \frac{d}{2}$, or on a negatively charged particle at the opposite edge $x - x_0 = -\frac{d}{2}$. The force and the particle energy enter equation (1) only in the ratio

$$\frac{E}{F_{max}} = R_c; \quad (2)$$

known as the critical radius [4].

Upon the bending of the crystal, the only change to Eq. (1) is that x_0 becomes a function of z coordinate, which for ultra-relativistic motion under small angles to Oz may be equated to the current time. In application to volume reflection, we are interested in the uniform bending of the crystal, at which $x_0(z)$ describes a circular arc of a small opening angle. That small arc may be approximated by a parabola, and then it is obvious that $x_0(t)$ is described by the equation

$$x_0(t) = x_0 + \frac{t^2}{2R}; \quad (3)$$

where R is the crystal bending radius. It will be convenient to introduce a shorthand for the inverse frequency of particle oscillations in the interplanar channel: $\omega = \frac{Ed}{2F_{max}} (2\pi$ is the period). Then, the particle equation of motion in the first interplanar interval appears as

$$x = \frac{1}{2} (x_0 + \frac{t^2}{2R}) \pm \frac{t}{\omega} \quad \begin{array}{l} \text{pos: ch: part:} \\ \text{neg: ch: part:} \end{array} \quad (4)$$

Initial conditions for $x(t)$ stand as

$$x(0) = b; \quad (5)$$

$$\dot{x}(0) = 0; \quad (6)$$

The equations of motion simplify in terms of the "subtracted radius" variable

$$r = x - x_0 + \frac{t^2}{2R}; \quad (7)$$

becoming

$$r = \frac{r}{2} \pm \frac{d}{2} \pm r \pm \frac{d}{2}; \quad (8)$$

where $\pm = \frac{2}{R}$. Hence, r is the spatial shift of the potential minimum position due to the bend of the crystal, i. e., due to the centrifugal force, which in the present small-angle approximation is regarded as independent of the radius (cf. [1]). For $r(t)$, the initial conditions (5-6) turn to

$$r(0) = b; \quad (9)$$

$$\dot{r}(0) = 0; \quad (10)$$

Eq. (8) describes a conservative harmonic oscillator with shifted equilibrium position, whose general solution is

$$r = A_0 \frac{\sin \frac{t}{\omega} + r_0}{\sinh \frac{t}{\omega}}; \quad (11)$$

Matching initial conditions (9-10) determines constants A_0 and r_0 :

$$A_0 = \frac{q}{2 \frac{2}{0} (b \frac{3}{j});} \quad (12)$$

$$r_0 = \frac{\arcsin \frac{b}{A_0}}{\text{arsinh} \frac{b}{A_0}}; \quad (13)$$

If $r_0 \ll d$, A_0 depends on b weakly, therefore the spread of reflection angles is anticipated to be much less than its mean value.

B. Connection of solutions in adjacent intervals

The particle reaches the boundary of the initial interval at a time

$$\frac{t_1}{\omega} = \frac{\arcsin \frac{d}{2} + r_0}{\text{arsinh} \frac{d}{2} + A_0}; \quad (14)$$

Thereupon, its equation of motion changes to

$$r = \frac{(d+r)}{2} \pm \frac{3d}{2} \pm r \pm \frac{d}{2}; \quad (15)$$

This is again a harmonic oscillator, only with a changed position of the equilibrium, thus

$$r_1(t) = d \pm \frac{\sin \frac{t}{\omega} + r_0 + 4r_1}{\sinh \frac{t}{\omega}}; \quad (16)$$

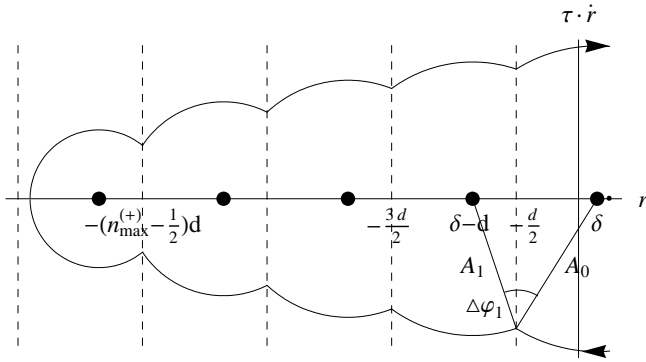


FIG. 2: The phase space trajectory for positively charged particles, under conditions $\frac{d}{2} > \dots$. Angle ϕ'_1 may be interpreted as a geometric sum of angles in adjacent right triangles with known legs $\frac{d}{2} + \dots, \frac{d}{2}$, and the hypotenuses A_0, A_1 .

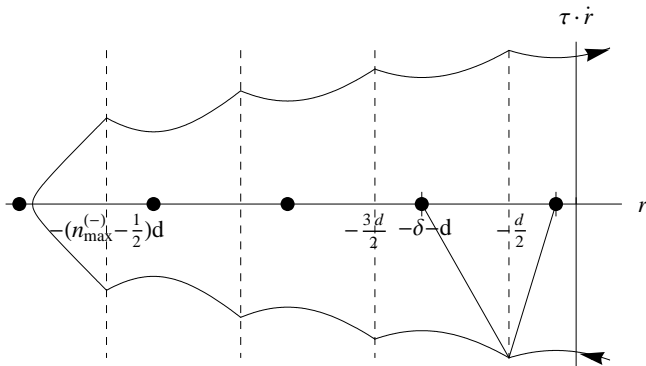


FIG. 3: The same as Fig. 2, but for negatively charged particles.

Values of constants A_1, ϕ'_1 are now to be determined from the continuity of $r(t)$ and $\dot{r}(t)$ in the boundary point $r = \frac{d}{2}$. In the first place, one must observe the relation between the amplitudes, not involving the initial phase, and being basically the result of energy conservation in the potential field:

$$A_1^2 = \frac{2}{\epsilon_1} r_1^2 \quad \left(\quad d \quad \right)^2 = A_0^2 \quad 2d: \quad (17)$$

Hence,

$$A_1 = \frac{q}{A_0^2} \quad 2d: \quad (18)$$

Secondly, ϕ'_1 is sought from $r(t)$ continuity at $r = \frac{d}{2}$. Equating the times expressed from Eqs. (11) and (16), one finds

$$\phi'_1 = \frac{\arcsin \frac{d}{2}}{\operatorname{arsinh} \frac{d}{A_0}} - \frac{\arcsin \frac{d}{2}}{\operatorname{arsinh} \frac{d}{A_1}} \quad (19)$$

(for geometric derivation of this relation { see Fig. 2). Note that ϕ'_1 is independent of ϕ_0 , too.

The beneficial property of harmonic oscillator is that its amplitude in each inter-planar interval depends only

on the amplitude in the previous interval. That allows one to evaluate amplitude in an arbitrary interval by induction:

$$A_n = \frac{q}{A_0^2} \quad 2nd = \frac{q}{A_0^2} \quad 2nd: \quad (20)$$

Furthermore, the phase shift at a boundary crossing depends only on the amplitudes in the neighboring intervals, but granted that those amplitudes are already known, and we can utilize them for expressing the phase shift at generic n :

$$\phi'_n = \frac{\arcsin \frac{d}{2}}{\operatorname{arsinh} \frac{d}{A_{n-1}}} - \frac{\arcsin \frac{d}{2}}{\operatorname{arsinh} \frac{d}{A_n}}: \quad (21)$$

As a whole, the particle trajectory expresses as

$$r_n(t) = \frac{nd}{A} \frac{\sin \frac{t}{\tau} + \phi'_0 + \sum_{m=1}^N \phi'_m}{\sinh} : \quad (22)$$

$$\frac{d}{2} \quad nd \quad r \quad \frac{d}{2} \quad nd; \quad t_n \quad t \quad t_{n+1}$$

The instants of border passage can also be evaluated:

$$\frac{t_n}{\tau} = \sum_{m=1}^N \frac{\arcsin \frac{d}{2}}{\operatorname{arsinh} \frac{d}{A_{m-1}}} + \sum_{m=1}^{N-1} \frac{\arcsin \frac{d}{2}}{\operatorname{arsinh} \frac{d}{A_m}} - \frac{\arcsin \frac{d}{2}}{\operatorname{arsinh} \frac{d}{A_0}}: \quad (23)$$

Amplitudes A_n do not actually represent the magnitude of particle wiggling { since the period 2π is much greater than the time of passage through an interval, the particle is far from making a full oscillation during its passage through an interval, anyway. As Figs. 2,3 indicate, the trajectory swings amplitudes as the particle enters deeper into the crystal, but thereat amplitudes A_n decrease. In fact, it is their decrease which allows the trajectory to bend and wiggle stronger.

III. VOLUME REFLECTION PHENOMENON

A. Reflection conditions for positive particles

It is clear that the decrease of amplitudes (20) can not continue infinitely, because eventually arguments of arcsines in (21) will exceed unity. This means that the particle can not reach the next inter-planar interval. It will continue the oscillatory motion until it hits the previous interval, then it will move outwards in the radial variable in the same but reverse way, and on the exit from the crystal it will emerge as a detected beam.

Let us evaluate the order number $n_{\max}^{(+)}$ of the reflection interval. If for some inequality $\frac{d}{2} + \dots A_{n-1}$ holds, then

it also entails $\frac{d}{2} < A_0$, so arguments of both arcsines in (23) are less than unity. So, $n_{m \text{ ax}}^{(+)}$ is the largest integer for which $\frac{d}{2} < A_{n_{m \text{ ax}}^{(+)}}$. This determines the radiation interval:

$$n_{m \text{ ax}}^{(+)} = \left\lfloor \frac{\sqrt{\frac{d^2}{4} + (b + \frac{d}{2})^2}}{2d} \right\rfloor \quad (24)$$

with the lower-comer brackets $\lfloor \cdot \rfloor$ indicating the integer part of a number. If $\frac{d}{2} > d$, then variation of $n_{m \text{ ax}}^{(+)}$ is much smaller than its mean value

$$n_{m \text{ ax}} \approx \frac{\sqrt{\frac{d^2}{4} + (b + \frac{d}{2})^2}}{2d} \quad (25)$$

We are interested in the total reflection angle α_{re} , half of which, by symmetry reasons, is the deflection angle in the reflection point:

$$\frac{1}{2} \alpha_{re} = \alpha(\tau_{re}) = \alpha_0 + \frac{\tau_{re}}{2} \quad (26)$$

To evaluate the right-hand side, we only need to know τ_{re} . The latter is found from solving $\underline{r}(\tau_{re}) = 0$:

$$\begin{aligned} \tau_{re} &= \frac{\tau_{n_{m \text{ ax}}^{(+)}}}{2} + \frac{1}{2} \sum_{n=1}^{n_{m \text{ ax}}^{(+)}-1} \arcsin \frac{\frac{d}{2} + \frac{d}{2(n+1)}}{A_n} + \arcsin \frac{\frac{d}{2}}{A_{n_{m \text{ ax}}^{(+)}}} \\ &= \arcsin \frac{b + \frac{d}{2}}{A_0} \quad (27) \end{aligned}$$

The largest contribution to this sum comes from terms $n = n_{m \text{ ax}}^{(+)}$ (where denominators A_n are the smallest), so it may be more convenient to carry out the summation in the inverse order. Introducing [9]

$$\tau_{n_{m \text{ ax}}^{(+)}} = \left(\frac{\sqrt{\frac{d^2}{4} + (b + \frac{d}{2})^2}}{2d} - \frac{d}{2} \right) \quad (28)$$

with braces $\{ \cdot \}$ to indicate the fractional part ($0 < \{ \cdot \} < 1$), one rewrites (27) as

$$\begin{aligned} \tau_{re} &= \frac{1}{2} \arcsin \frac{b + \frac{d}{2}}{\sqrt{\frac{d^2}{4} + 2\{ \frac{d}{2} + \frac{d}{2(n_{m \text{ ax}}^{(+)} + 1) \} d}} \\ &+ \sum_{n=0}^{n_{m \text{ ax}}^{(+)}-1} \arcsin \frac{\frac{d}{2} + \frac{d}{2(n+1)}}{\sqrt{\frac{d^2}{4} + 2\{ \frac{d}{2} + \frac{d}{2(n+1) \} d}} \\ &+ \arcsin \frac{\frac{d}{2}}{\sqrt{\frac{d^2}{4} + 2\{ \frac{d}{2} + \frac{d}{2(n_{m \text{ ax}}^{(+)} + 1) \} d}} \quad (29a) \end{aligned}$$

Equivalently, using the identity $\arcsin \frac{1}{1+x} = \arccot \sqrt{x}$,

one can write

$$\begin{aligned} \tau_{re} &= \frac{1}{2} \arcsin \frac{b + \frac{d}{2}}{\sqrt{\frac{d^2}{4} + 2\{ \frac{d}{2} + \frac{d}{2(n_{m \text{ ax}}^{(+)} + 1) \} d}} \\ &+ \sum_{n=0}^{n_{m \text{ ax}}^{(+)}-1} \arccot \sqrt{\frac{\frac{d}{2} + \frac{d}{2(n+1)}}{\frac{d}{2} + \frac{d}{2(n+1)}}} + \arccot \sqrt{\frac{\frac{d}{2}}{\frac{d}{2} + \frac{d}{2(n_{m \text{ ax}}^{(+)} + 1)}}} \quad (29b) \end{aligned}$$

B. Negative particles

An arc-hyperbolic sine function exists at any value of the argument. Therefore, Eq. (22) for negative particle trajectories holds until the radicand in amplitude (20) becomes negative. This entails for the order number of the reflection interval

$$n_{in} = \left\lfloor \frac{\sqrt{\frac{d^2}{4} + (b - \frac{d}{2})^2}}{2d} \right\rfloor + 1 \quad (30)$$

In the reflection interval, the amplitude $A_{n_{in}}$, calculated by the formula (20), would be imaginary. That means that the $r(t)$ dependence is described rather by a hyperbolic cosine, not a sine (see Fig. 3). The connection of the amplitude and phase of the hyperbolic cosine with solution (22) at $n = n_{in} - 1$ gives

$$\begin{aligned} r_{n_{in}}(t) &= A_{n_{in}} d + \tilde{A}_{n_{in}} j \cosh \left(\frac{t}{\tau_{n_{in}}} + \tau_{n_{in}} \right) + \sum_{m=1}^{n_{in}-1} \tilde{A}_{n_{in}} j \operatorname{arcsinh} \frac{\frac{d}{2}}{A_{n_{in}-1}} \operatorname{arccosh} \frac{\frac{d}{2} + \frac{d}{2(n_{in}-m)}}{\tilde{A}_{n_{in}-1}} ; \\ &\frac{d}{2} n_{in} d \quad r_{n_{in}} \quad \frac{d}{2} n_{in} d \quad (31) \end{aligned}$$

where

$$\tilde{A}_{n_{in}} j = \frac{q}{\sqrt{\frac{d^2}{4} + (b - \frac{d}{2})^2 + 2n_{in} d}} \quad (32)$$

with [10]

$$\tau_{n_{in}} = \frac{\sqrt{\frac{d^2}{4} + (b - \frac{d}{2})^2}}{2d} \quad (33)$$

Since $\frac{d}{2} + \frac{d}{2} > 1$, the argument of arccosh in (31) is automatically > 1 .

Next, a question arises, whether trajectory (31) can reach the next interval. That would require a condition

$$\frac{d}{2} > \tilde{A}_{n_{in}} j \quad (34)$$

If

$$\frac{d}{2} > \frac{q}{2} \quad (35)$$

then at least for (γ) sufficiently close to 1 Eq. (34) will hold.

If condition (35) is not satisfied, then (30) is the last interval reached by the particle, and

$$n_{max}^{(\gamma)} = n_{in} = \frac{\sqrt{\frac{2}{0} (b \gamma)} + 1}{2d} : \frac{d}{2} \quad (36)$$

Expressing t_{re} from equation $r(t_{re}) = 0$,

$$\frac{t_{re}}{c} = \text{arccosh} \frac{\frac{d}{2} + \sum_{n=1}^{n_{in}} \frac{b}{A_n j}}{\sum_{n=1}^{n_{in}} \frac{b}{A_n j}} \text{arsinh} \frac{b}{A_0} + \sum_{n=0}^{n_{in}-1} \text{arsinh} \frac{\frac{d}{2}}{A_n} + \sum_{n=1}^{n_{in}-1} \text{arsinh} \frac{\frac{d}{2} + b}{A_n} : \quad (37)$$

Change of the summation order here leads to the expression

$$\frac{t_{re}}{c} = \text{arccosh} \frac{\frac{d}{2} + \sum_{n=0}^{n_{in}-1} \frac{b}{2d(1+\gamma)^n}}{\sum_{n=0}^{n_{in}-1} \frac{b}{2d(1+\gamma)^n}} \text{arsinh} \frac{b}{A_0} + \sum_{n=0}^{n_{in}-1} \text{arsinh} \frac{\frac{d}{2}}{2d(1+\gamma)^n} + \sum_{n=0}^{n_{in}-2} \text{arsinh} \frac{\frac{d}{2} + b}{2d(1+\gamma)^{n+1}} ; \quad (38)$$

Therefore, by Eq. (26) results the deflection angle.

Otherwise, i. e. if (34) holds for a given (γ) , in the intervals beyond (30) the trajectory must again express through a hyperbolic cosine:

$$r_n(t) = nd + \sum_{m=1}^{n_{in}} \frac{b}{A_m j} \text{cosh} \frac{t}{c} + \sum_{m=1}^{n_{in}} \frac{b}{A_m j} \text{arsinh} \frac{\frac{d}{2}}{A_{n_{in}-m+1}} \text{arccosh} \frac{\frac{d}{2} + \sum_{m=n_{in}-m+1}^{n_{in}} \frac{b}{A_m j}}{\sum_{m=n_{in}-m+1}^{n_{in}} \frac{b}{A_m j}} + \sum_{m=n_{in}-m+1}^{n_{in}} \frac{b}{A_m j} \text{arccosh} \frac{\frac{d}{2} + b}{A_m j} : \quad (39)$$

$$\frac{d}{2} \quad nd \quad \frac{d}{2} \quad nd; \quad n \quad n_{in}$$

This sequence can continue until

$$\frac{d}{2} + \sum_{n=1}^{n_{in}} \frac{b}{A_n j} \quad (40)$$

(which is equivalent to $\frac{d}{2} + \sum_{n=1}^{n_{in}} \frac{b}{A_n j}$). That yields for the order number of the reflection interval

$$n_{max}^{(\gamma)} = \frac{\sqrt{\frac{2}{0} (b \gamma)} + \frac{d}{2} + \sum_{n=1}^{n_{in}} \frac{b}{A_n j}}{2d} : \frac{d}{2} \quad (41)$$

(cf. Eq. (24)). As one might expect, in the high-energy limit these two expressions coincide and do not depend on the particle energy).

Then,

$$\frac{t_{re}}{c} = \text{arsinh} \frac{b}{A_0} + \sum_{n=0}^{n_{in}-1} \text{arsinh} \frac{\frac{d}{2}}{A_n} + \sum_{n=1}^{n_{in}-1} \text{arsinh} \frac{\frac{d}{2} + b}{A_n} : \quad (42)$$

$$+ \sum_{m=n_{in}}^{n_{max}^{(\gamma)}} \text{arccosh} \frac{\frac{d}{2} + \sum_{m=n_{in}-m+1}^{n_{in}} \frac{b}{A_m j}}{\sum_{m=n_{in}-m+1}^{n_{in}} \frac{b}{A_m j}} \text{arccosh} \frac{\frac{d}{2} + b}{A_m j} + \sum_{m=n_{in}}^{n_{max}^{(\gamma)}} \text{arccosh} \frac{\frac{d}{2} + b}{A_m j} + \sum_{n=1}^{n_{in}-1} \text{arcsinh} \frac{b}{2d(n_{in}-1+\gamma)^n} + \sum_{n=0}^{n_{in}-1} \text{arcsinh} \frac{\frac{d}{2}}{2d(1+\gamma)^n} + \sum_{n=0}^{n_{in}-2} \text{arcsinh} \frac{\frac{d}{2} + b}{2d(1+\gamma)^{n+1}} ; \quad (43)$$

$$+ \sum_{n=1}^{n_{max}^{(\gamma)}} \text{arcsinh} \frac{\frac{d}{2} + b}{2d(1+\gamma)^n} : \quad (43)$$

Note that if one uses here

$$n_{max}^{(\gamma)} = \frac{\sqrt{\frac{2}{0} (b \gamma)} + \frac{d}{2} + \sum_{n=1}^{n_{in}} \frac{b}{A_n j}}{2d} + 1 ; \quad (44)$$

with (v) the Heavyside unit-step function, then Eq. (42-43) will be valid as well at $\gamma < \frac{d}{2}$, reproducing result (38).

C. Reflection angle in a thick crystal

Usually, the crystal may be regarded as thick, whence edge effects ought to fade out. Then,

$$\frac{1}{2} t_{re} = \lim_{c \rightarrow \infty} \frac{1}{2} v_{re} = \lim_{c \rightarrow \infty} \left(\frac{t_{re}(0)}{2} + \dots \right) : \quad (45)$$

This limit with function (29a), or (42), always exists, because at large n_{max} the sum grows as the corresponding integral, whose asymptotic behavior readily evaluates as

$$\frac{t_{re}}{c} \sim \int_{n_{max}}^{\infty} \frac{dn}{2(n+d)} + \int_{n_{max}}^{\infty} \frac{dn}{2(n+d)} \sim \frac{1}{2n_{max}d} , \quad 0^- :$$

This leading asymptotic behavior cancels with the first term in (45), and calculation of the finite remainder requires a more accurate estimation of the sum. That will be the subject of our study in the next section.

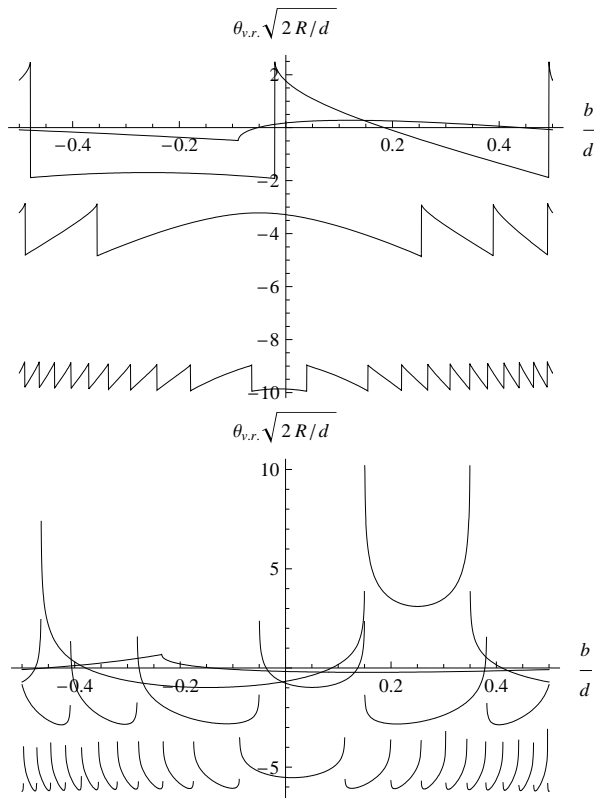


FIG. 4: The volume reflection angle as a function of impact parameter, for $R=R_c = 1; 3; 10; 40$. Upper panel { positively charged particles, lower panel { negatively charged particles.

Function $\theta_{v,r}(\xi; d; b)$, being a dimensionless quantity, depends only on three dimensionless ratios: say, $d = \frac{r}{R}$, $\xi = \frac{b}{d}$, $b = d \xi$. The last one of them is always 1. The first one,

$$\frac{d}{R} = \frac{r}{R} \frac{1}{E} = 2 \xi c; \quad (46)$$

where c is Lindhard's critical angle, is always small. As for the ratio

$$\frac{2}{d} = \frac{E}{F_{max} R} = \frac{R_c}{R}; \quad (47)$$

it can be either large or small depending on the particle energy and the crystal bending radius. The regime of particle passage through the crystal is determined by ratio (47) above.

Fig. 4 shows the dependence of the volume reflection angle on the impact parameter for positive and negative particles. For negative particles there are noticeable spikes of the reflection angle towards positive direction. That corresponds to close matching the energy of a parabolic potential barrier. The asymptotics of the spikes is logarithmic, in accord with the general integral

expression of the deflection angle in a central potential $V(r)$:

$$\begin{aligned} & \int_{r_{min}}^{r_{max}} \frac{dr}{r^2 \sqrt{(E - V(r))^2 - M^2/r^2}} \\ &= 2M \int_{r_{min}}^{r_{max}} \frac{dr}{r^2 \sqrt{(E - V(r))^2 - M^2/r^2}} \\ &= \frac{4}{c} \int_{r_{min}}^{r_{max}} \frac{dr}{2 \sqrt{4b + (r - r_{saddle})^2}} + \dots \quad (48a) \\ &= \frac{4}{c} \left(\ln \frac{2 \sqrt{4b} + r}{d} + \dots \quad 4b > 0 \right. \\ & \quad \left. \frac{1}{2} \ln \frac{2 \sqrt{4b}}{d} + \dots \quad 4b < 0 \right) \quad (48b) \end{aligned}$$

where r_{saddle} is the position of the potential barrier whose height is close to the particle energy, and the integration in (48a) carried out over the vicinity of r_{saddle} where the radicand is positive. In contrast, for positive particles, the force does not vanish at the top of the barrier (provided we neglect the thermal smearing of the potential), and instead of spikes there are only finite discontinuities of the reflection angle.

IV. MODERATE ENERGIES, LARGE BENDING RADIUS ($R \gg R_c$)

A. Positive particles

In the limiting case $d \ll 1$, it is possible to replace the summation in (27) by integration, because quantity $\frac{d}{2} \sqrt{2 + 2 \cos(\theta)} + n$ entering A_n varies relatively little at each summation step.

Applying for approximation of each of the sums in (29b) the Euler-Maclaurin formula [7]

$$\sum_{n=0}^N f(n) = \int_0^N f(n) dn + \frac{1}{2} f(0) + \frac{1}{2} f(N) + O\left(\frac{df}{dn}\right); \quad (49)$$

we get

$$\begin{aligned} & \sum_{n=0}^{n_{max}^{(+)}} \arcsin \frac{1}{1 + \frac{2d}{(\frac{d}{2})^2} \cos(\theta) + n} \\ &= \int_{n_{max}^{(+)}}^{n_{max}^{(+)}} \arcsin \frac{1}{1 + \frac{2d}{(\frac{d}{2})^2} \cos(\theta) + n} dn \\ &+ \frac{1}{2} \arcsin \frac{1}{1 + \frac{2d}{(\frac{d}{2})^2} \cos(\theta)} \\ &+ \frac{1}{2} \arcsin \frac{1}{1 + \frac{2d}{(\frac{d}{2})^2} \cos(\theta) + n_{max}^{(+)}} + O\left(\frac{dr}{d}\right) \quad (50) \end{aligned}$$

where we had estimated

$$\frac{d}{dn} \arcsin \frac{1}{1 + \frac{2d}{(\frac{d}{2})^2} \cos(\theta) + n} \sim \frac{r}{d}; \quad (51)$$

The two end-point contributions are small as $O(\epsilon/d)$ relative to the integral, but still they need to be kept if we wish also to describe not only the mean deflection, but also the scattered beam shape.

Taking the indefinite integral by parts

$$\int \frac{1}{1+an} \arcsin \frac{1}{1+an} = \frac{1}{a} (1+an) \arcsin \frac{1}{1+an} + \frac{p}{an};$$

we bring (50) to the form

$$\begin{aligned} & \sum_{n=0}^{n_{\text{max}}^{(+)}-1} \frac{1}{1 + \frac{2d}{(\frac{d}{2})^2} (n^{(+)} + n)} \arcsin \frac{1}{1 + \frac{2d}{(\frac{d}{2})^2} (n^{(+)} + n)} \\ & \frac{d}{2d} \left(1 + \frac{2d}{\frac{d}{2}} n_{\text{max}}^{(+)} + n^{(+)} \right) \\ & \arcsin \frac{1}{1 + \frac{2d}{(\frac{d}{2})^2} n_{\text{max}}^{(+)} + n^{(+)} - 1} \\ & + \frac{2d}{\frac{d}{2}} n_{\text{max}}^{(+)} + n^{(+)} - 1 \\ & \left(1 + \frac{2d}{\frac{d}{2}} n^{(+)} \right) \arcsin \frac{1}{1 + \frac{2d}{(\frac{d}{2})^2} n^{(+)} + \frac{p}{2d} n^{(+)}} \\ & + \frac{1}{2} \arcsin \frac{1}{1 + \frac{2d}{(\frac{d}{2})^2} n^{(+)}} \\ & + \frac{1}{2} \arcsin \frac{1}{1 + \frac{2d}{(\frac{d}{2})^2} n_{\text{max}}^{(+)} + n^{(+)} - 1} + O\left(\frac{1}{d}\right) \end{aligned} \quad (52)$$

Proceeding to limit $n_{\text{max}}^{(+)} \rightarrow \infty$ with the use of expansion $\arcsin \frac{1}{1+a} = \frac{1}{2} \left(\frac{1}{1+a} + O\left(\frac{1}{3+2a}\right) \right)$,

$$\begin{aligned} & \sum_{n=0}^{n_{\text{max}}^{(+)}-1} \frac{1}{1 + \frac{2d}{(\frac{d}{2})^2} (n^{(+)} + n)} \arcsin \frac{1}{1 + \frac{2d}{(\frac{d}{2})^2} (n^{(+)} + n)} \\ & \frac{d}{2d} \left(1 + \frac{2d}{\frac{d}{2}} n_{\text{max}}^{(+)} + n^{(+)} \right) \\ & \frac{1}{2} \left(\frac{1}{1 + \frac{2d}{(\frac{d}{2})^2} n_{\text{max}}^{(+)} + n^{(+)} - 1} + \frac{1}{1 + \frac{2d}{(\frac{d}{2})^2} n^{(+)} + \frac{p}{2d} n^{(+)}} \right) \\ & + \frac{1}{2} \left(\frac{1}{1 + \frac{2d}{(\frac{d}{2})^2} n^{(+)}} + \frac{1}{1 + \frac{2d}{(\frac{d}{2})^2} n_{\text{max}}^{(+)} + n^{(+)} - 1} \right); \end{aligned} \quad (53)$$

One can see that terms $\frac{1}{d} \left(\frac{1}{1 + \frac{2d}{(\frac{d}{2})^2} n_{\text{max}}^{(+)} + n^{(+)} - 1} \right)$ cancel there. Further on, substituting (53) to (29a) and this to (45), we witness

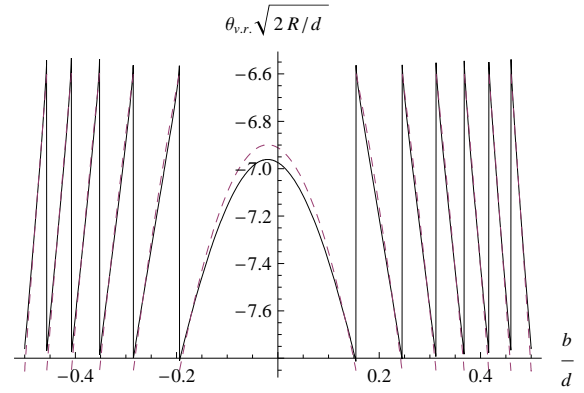


FIG. 5: Comparison of the exact volume reflection indicatrix (45, 29a) (solid line) with the approximation (54) (dashed line), for $R=R_c = 25$.

the cancellation of large terms $\frac{1}{2} \left(\frac{1}{1 + \frac{2d}{(\frac{d}{2})^2} n_{\text{max}}^{(+)} + n^{(+)} - 1} \right) = 0$, and ultimately obtain the finite result

$$\begin{aligned} & \frac{d}{2d} \left(1 + \frac{2d}{\frac{d}{2}} n_{\text{max}}^{(+)} + n^{(+)} \right) \\ & \frac{1}{2} \left(\frac{1}{1 + \frac{2d}{(\frac{d}{2})^2} n_{\text{max}}^{(+)} + n^{(+)} - 1} + \frac{1}{1 + \frac{2d}{(\frac{d}{2})^2} n^{(+)} + \frac{p}{2d} n^{(+)}} \right) \\ & + \frac{1}{2} \left(\frac{1}{1 + \frac{2d}{(\frac{d}{2})^2} n^{(+)}} + \frac{1}{1 + \frac{2d}{(\frac{d}{2})^2} n_{\text{max}}^{(+)} + n^{(+)} - 1} \right) \\ & = \frac{1}{2} \left(1 + \frac{8}{d} n^{(+)} \right) \left(1 + O\left(\frac{1}{d^{3-2}}\right) \right); \end{aligned} \quad (54)$$

Comparison of the approximation (54) with the exact result is shown in Fig. 5. It appears to be numerically accurate down to $R=R_c = 5$. Basically, in this limit the angular distribution acquired by the detected beam is table-shaped, of the full width $\frac{4}{d}$, which more precisely will be discussed below.

a. Differential cross-section For asymptotic dependence (54), it is not difficult to explicitly express the angular distribution function in angles (i.e., the scattering differential cross-section, if one assumes equiprobable distribution of the incoming particles in impact parameters. The differential cross-section (in 1d case having a dimension of length) expresses through the scattering indicatrix (b) by the formula

$$\frac{d}{d_{\text{v.r.}}} = \sum_{m=1}^X \frac{1}{|j_{\text{v.r.}}(b) - j_{\text{v.r.}}(b_m)|}; \quad (55)$$

where b_m are all the roots of the equation (b) = 0 on the interval $\frac{d}{2} < b < \frac{d}{2}$.

To find those roots, observe that we can explicitly express $n^{(+)}$ from (54)

$$n^{(+)}(v.r.) = 1 - \frac{2}{c} v.r. + 1 - \frac{d}{8}; \quad (56)$$

On the other hand, from definition (28) we can express b through $n^{(+)}$ and thereby obtain an explicit expression

for b through v_{ir} . Eq. (28) is equivalent to

$$\frac{2 \frac{2}{0} + (b + \frac{d}{2})^2}{2 d} = (+) + m$$

with m an integer number, whereby the solutions of Eq.

$$v_{ir}(b) = v_{ir}$$

$$b_m = \sqrt{2 d (+) (v_{ir}) + m + \frac{d}{2}} \quad (57)$$

The sequence of m begins with a smallest integer m_0 at which the radicand in (57) is positive, viz.

$$m_0 = \frac{2 \frac{2}{0} + \frac{d}{2}}{2 d} (+) (v_{ir}) + 1 \quad (58)$$

The upper limit of m equals to the largest integer at which $b < \frac{d}{2}$ (for a branch with "+" sign in front of the root in Eq. (57)), and $b > \frac{d}{2}$ (for a branch with "-" sign). That yields, correspondingly, values

$$m_{max1} = \frac{2 \frac{2}{0}}{2 d} (+) (v_{ir}) \quad (59)$$

$$m_{max2} = m_{max1} + 1 \quad (60)$$

Values of derivative $\frac{d v_{ir}}{db}$ in points b_m are easily evaluated, noting that the fractional part operation in (+) is inconsequential thereat. Differentiating gives

$$\begin{aligned} \frac{d v_{ir}}{db} \Big|_{b=b_m} &= \frac{4 c}{d} \frac{d}{db} \frac{2 \frac{2}{0} + (b + \frac{d}{2})^2}{2 d} \Big|_{b=b_m} \\ &= \frac{4 c}{d^2} (b_m + \frac{d}{2}) \end{aligned} \quad (61)$$

Therefore, through (57, 55), the differential cross-section is

$$\begin{aligned} \frac{d}{d v_{ir}} &= \frac{S}{4 c} \frac{d^2}{2 d \frac{(\frac{d}{2})^2} + \frac{d}{8} \frac{2 v_{ir}}{c} + 1} \\ + \sum_{m=0}^{m_{max1} m_0} \frac{d^2}{2 c} \frac{d^2}{2 d m + 1 \frac{2 \frac{2}{0} + (\frac{d}{2})^2}{2 d} + \frac{d}{8} \frac{2 v_{ir}}{c} + 1} \end{aligned} ;$$

if

$$\frac{2}{c} < v_{ir} < \frac{2}{c} + 1 \frac{8}{d} \quad (63)$$

and zero otherwise. The first term in (64) is $O(\frac{d}{d})$ relative to the sum and is beyond our accuracy $O(\frac{1}{d})$.

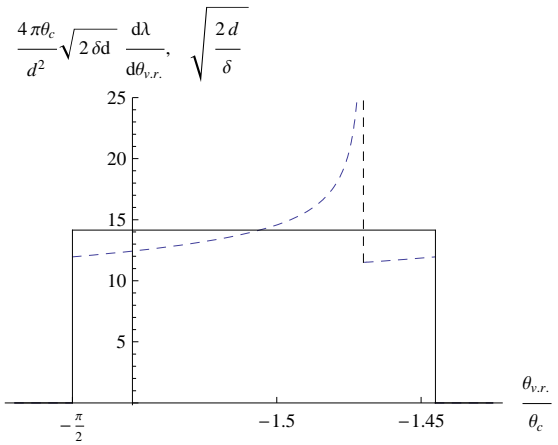


FIG. 6: A symptotic behavior of the differential cross-section, plotted for $R=R_c = 25$. Dashed { for a certain θ_0 , solid { averaged over θ_0 . In higher orders in d the distribution edges smear out.

Dropping it and making a simplification under the sum sign,

$$\frac{d}{d v_{ir}} = \frac{m_{max1} m_0}{m=0} \frac{d^2}{2 c} \frac{d^2}{2 d m + 1 \frac{2 \frac{2}{0} + \frac{d}{4} \frac{v_{ir}}{c}}}} \quad (64)$$

That distribution is shown in Fig. 6. Apparently, it has a noticeable cusp [11] at

$$\frac{2 \frac{2}{0}}{2 d} + \frac{d}{4} \frac{v_{ir}}{c} = 0 \quad (65)$$

which is still dependent on θ_0 despite the thick-crystal limit $\theta_0 \ll 1$. However, the dependence on θ_0 here is quadratic, and with a statistical angular indeterminacy in the incident particle beam, even smaller than the scattering angle scale c ,

$$\frac{2}{c} = \frac{d}{2} \frac{4}{d} c = \frac{2}{R} = 2 \frac{r}{R} \quad (66)$$

the cusp position may be equiprobable in the interval (63). Then,

$$\frac{d}{d v_{ir}} = \frac{d^2}{4 c} \quad (67)$$

The latter relation may be obtained from (64) by straightforward averaging over θ_0 , as well as from Eq. (54) through

$$\frac{d}{d v_{ir}} = \sum_k \frac{d}{d v_{ir} = d^{(k)}(v_{ir})} \quad (68)$$

(the sum over all the roots of equation $v_{ir}^{(k)} = v_{ir}$), which is a consequence of nearly linear (b) dependence in each small continuity interval.

However, in existing experiments on volume reflection the right-hand side inequality of (66) does not hold, and then, the angular spread due to interaction with the continuous potential may be neglected as compared to the initial beam width, and with the spread due to multiple scattering on individual target nuclei.

B. Negative particles

In the case of negative particles, we must issue from Eq. (38). Although at $n \rightarrow 1$ the argument of arcsines varies significantly, but the arcsine itself is similar to a logarithm of large argument, and varies relatively little. Thus, both entering sums, may be approximated by integrals. The first one of the sums, by the Euler-Maclaurin formula,

$$\sum_{n=0}^{n_{in}-1} \operatorname{arsinh} \frac{\frac{d}{2}}{p \frac{d}{2} + n} + \frac{1}{2} \operatorname{arsinh} \frac{\frac{d}{2}}{p \frac{d}{2} + n_{in}} + \frac{1}{2} \operatorname{arsinh} \frac{\frac{d}{2}}{p \frac{d}{2} + n_{in} - 1} \quad (69)$$

Calculating the indefinite integral by parts,

$$\int \operatorname{arsinh} \frac{a}{n} dn = n \operatorname{arsinh} \frac{a}{n} + a \sqrt{a^2 + n^2}; \quad (70)$$

we bring (69) to form

$$\sum_{n=0}^{n_{in}-1} \operatorname{arsinh} \frac{\frac{d}{2}}{p \frac{d}{2} + n} + \frac{1}{2} \operatorname{arsinh} \frac{\frac{d}{2}}{p \frac{d}{2} + n_{in}} + \frac{1}{2} \operatorname{arsinh} \frac{\frac{d}{2}}{p \frac{d}{2} + n_{in} - 1} + \frac{1}{2} \operatorname{arsinh} \frac{\frac{d}{2}}{p \frac{d}{2} + n_{in}} + \frac{1}{2} \operatorname{arsinh} \frac{\frac{d}{2}}{p \frac{d}{2} + n_{in} - 1} \quad (71)$$

Now, in the limit $n_{in} \rightarrow 1$,

$$\sum_{n=0}^{n_{in}-1} \operatorname{arsinh} \frac{\frac{d}{2}}{p \frac{d}{2} + n} + \frac{1}{2} \operatorname{arsinh} \frac{\frac{d}{2}}{p \frac{d}{2} + n_{in}} + \frac{1}{2} \operatorname{arsinh} \frac{\frac{d}{2}}{p \frac{d}{2} + n_{in} - 1} \quad (38)$$

Similarly, the second term in (38)

$$\sum_{n=0}^{n_{in}-2} \operatorname{arsinh} \frac{\frac{d}{2} + 1}{p \frac{d}{2} + n} + \frac{1}{2} \operatorname{arsinh} \frac{\frac{d}{2} + 1}{p \frac{d}{2} + n_{in} - 1} + \frac{1}{2} \operatorname{arsinh} \frac{\frac{d}{2} + 1}{p \frac{d}{2} + n_{in} - 2} \quad (45)$$

Substituting this to (38) and to (45),

$$\sigma_{\text{vol}} = \frac{2}{4} \frac{d}{d} \operatorname{arcsinh} \frac{\frac{d}{2} + 1}{p \frac{d}{2} + 1} + \dots + \frac{1}{2} \operatorname{arsinh} \frac{\frac{d}{2}}{p \frac{d}{2} + n_{in}} + \operatorname{arsinh} \frac{\frac{d}{2} + 1}{p \frac{d}{2} + n_{in}} \quad (72)$$

or, approximating the inverse hyperbolic functions of large arguments by logarithm,

$$\sigma_{\text{vol}} \approx \frac{4}{d} \frac{1}{2} \ln \frac{d}{2 \sqrt{1 + \dots}} + \frac{1}{2} \ln \frac{d}{2} \quad (73)$$

Logarithmic asymptotics of this expression at $n_{in} \rightarrow 0$ coincides with the generic law (48a). As for the asymptotics at $n_{in} \rightarrow 1$, which corresponds to approaching the potential barrier with a slightly excessive energy, the coefficient at the first logarithm in Eq. (73) is half that in Eq. (48a). This owes to inaccuracy of application of the Euler-Maclaurin formula at the edge of the summation interval, but this discrepancy at generally is practically unnoticeable { see Fig. 7.

b. Differential cross-section Computing the differential cross-section accounting for the θ_0 -dependent cusp position is more complicated for negative particles than for positive, because of the transcendental dependence $\sigma_{\text{vol}}(\theta_0)$. Let us limit ourselves to evaluating the

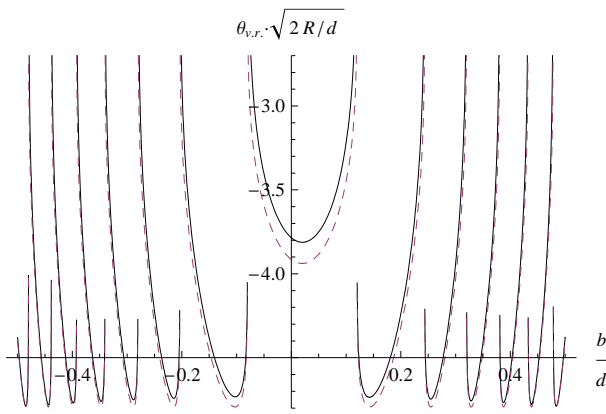


FIG. 7: Comparison of the exact formula (45, 38) (solid line) with the approximation (73) (dashed line) for $R=R_c = 25$.

0-averaged expression for the differential cross-section, based on formula (68). In the present case, equation $v_{vir}(\xi) = v_{vir}$ can not be solved explicitly but only within logarithmic accuracy, with different approximations in different regions.

The steepest dependence of v_{vir} on ξ is borne by the second term in (73), except in the domain of ξ close to 1, where the first logarithm becomes steep, too, and a minimum of function $v_{vir}(\xi)$ develops. The position of that minimum can be determined with logarithmic accuracy:

$$\xi_0 \approx 1 - \frac{1}{1 + 2 \ln \frac{d}{2}} \quad (74)$$

Expanding function $v_{vir}(\xi)$ in vicinity of ξ_0 up to the quadratic term

$$\frac{v_{vir}}{c} + 1 - \frac{d}{4} = \frac{1}{2} \ln \frac{2}{e} \ln \frac{d}{2} + \xi_0^2 \ln^2 \frac{d}{2} + O(\xi_0 - \xi_0^3); \quad (75)$$

one evaluates by formula (68) the behavior of the differential cross-section at the left edge:

$$\frac{c}{d} \frac{d}{d v_{vir}} = \frac{d}{4 \ln \frac{e^{1+2d}}{2} \left(\frac{v_{vir}}{c} + 1 - \frac{d}{4} - \frac{1}{2} \ln \frac{2}{e} \ln \frac{d}{2} \right)} \quad (76)$$

$$\frac{v_{vir}}{c} + 1 - \frac{4}{d} \ln^2 \frac{d}{2}$$

On the other hand, if ξ is not too close to 1, the first logarithm in (73) can be approximated by a linear function, through a Taylor expansion, e. g., in the vicinity of $\xi = \frac{1}{2}$:

$$\frac{1}{2} \ln \frac{1}{1 - \xi} = \frac{\ln 2}{2} + \xi + O(\xi^2) \quad (1=2^2):$$

Therefore, Eq. (73) becomes

$$\frac{v_{vir}}{c} + 1 - \frac{d}{4} = \frac{1}{2} \ln \frac{d}{e} + \frac{1}{2} \xi \ln \frac{d}{2} \quad (77)$$

To simplify it more, function $\xi \ln \xi$ from the last term may be substituted by its average value

$$\xi \ln \xi = \int_0^1 \xi \ln \xi d\xi = -\frac{1}{4}$$

Then, for determination of the inverse function $\xi(v_{vir})$ we obtain an equation

$$\frac{v_{vir}}{c} + 1 - \frac{d}{4} = \frac{1}{2} \ln \frac{d^2}{2e^{3+2\xi}} + \xi \ln \frac{d}{2} \quad (78)$$

The r. h. s. is a monotonic function of ξ , and its inverse expresses through a Lambert (product log) function $W(s)$ defined as a solution to the equation $s = W e^W$ at $s = 0$:

$$\xi = \frac{1}{2 \ln \frac{d}{2}} W \left(\frac{d^2 \ln \frac{d}{2}}{e^{3+2\xi}} e^{\frac{d}{2} \left(\frac{v_{vir}}{c} + 1 \right)} \right) \quad (79)$$

The asymptotics of W is

$$W(s) \approx \begin{cases} s & s \ll 1 \\ \ln \frac{s}{\ln s} & s \gg 1 \end{cases} \quad (80)$$

and its derivative

$$W'(s) = \frac{1}{s(1+W(s))}$$

Thus,

$$\frac{c}{d} \frac{d}{d v_{vir}} = \frac{d}{c} \frac{d \xi}{d v_{vir}} = \frac{d}{4 \ln \frac{d}{2} (1+W(s))} \quad (81)$$

The parts of the differential cross-section (76) and (81) are shown in Fig. 8.

The full width of the differential cross-section is inferred simply from Eq. (73):

$$4 v_{vir}' = \frac{4}{c} \ln \frac{d}{2} \quad (82)$$

However, at practice, as well as for positive particles, this width is usually smaller than that of the initial beam divergence.

V. HIGH-ENERGY LIMIT (PERTURBATIVE SCATTERING)

In conclusion, we will briefly comment on dependence $v_{vir}(\theta)$ in the opposite limit,

$$\frac{d}{2} = \frac{R}{R_c} \quad (1): \quad (83)$$

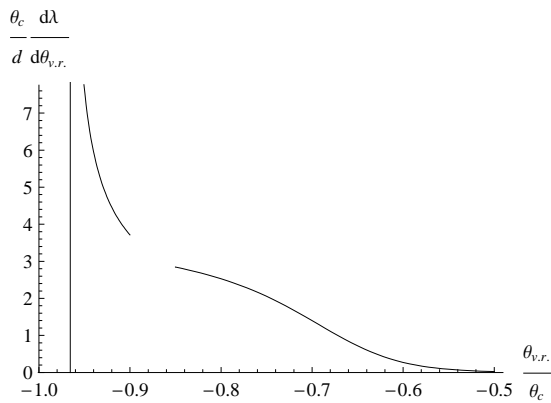


FIG. 8: θ_c -averaged differential cross-section at $R=R_c = 25$. The left-hand curve is evaluated by formula (76), the right-hand curve { by formula (81).

Obviously, since R_c , are proportional to the particle energy, condition (83) is equivalent to the high-energy limit. Thereat, the deflection is perturbative (and better viewed in Cartesian coordinates), and for positive and negative particles it must be equal in magnitude but opposite in sign. This is confirmed by Figs. 4.

The expression for the dependence $\nu_{v,r}(b)$ in this limit has been obtained in [6], in the Cartesian coordinate framework. It involves a Hurwitz (generalized Riemann) zeta-function. Reproducing that formula from Eqs. (29a, 43) may again proceed through replacement of summation by integration, but this time the Euler-Maclaurin formula is insufficient, and one must use the Abel-Plan

formula with a contour integral representation for the remainder term [7]. Since this subject appears to be mathematically involved, we refrain from discussing it here.

V I. S U M M A R Y

In this paper, within the model of a purely parabolic inter-planar potential, an explicit analytic expression (22) was obtained for the trajectory of the passing particle, for positive and negative sign of particle charge. On its basis, expressions are derived for the particle final deflection angle as a function of impact parameter, in the form of functional series (29a, 38, 43). A asymptotic behavior of this series at $R \rightarrow R_c$ was investigated, and asymptotic values for the volume reflection angle were found. They equal: $\frac{\pi}{2} - \epsilon$ for positive particles, and $\frac{\pi}{2} + \epsilon$ for negative particles (in accord with the existing estimates obtained by numerical simulation). Also, estimates for the final particle beam width and shape were obtained.

The outlined theory may serve as a basis for description of processes occurring at interaction of fast positively and negatively charged particles with bent silicon crystals in orientation (110). Other effects, such as potential departure from parabolicity, incoherent scattering, etc. may be introduced in a perturbative manner. There still remains a problem to extend the present formulation to the case of (111) orientation, which involves alternating parabolic potential wells of different depth.

[1] A. M. Taratin and S. A. Vorobiev. NIM B 26 (1987) 512-521.
 [2] A. M. Taratin. Phys. Part. Nucl. 29 (1998) 437; A. M. Taratin, W. Scandale. NIM B 262 (2007) 340.
 [3] V. A. M. Aisheev. Phys. Rev. ST 10 (2007) 084701.
 [4] E. N. Tsyganov, Fermilab Report No. TM-682, 1976 (unpublished); Fermilab Report No. TM-684, 1976 (unpublished).
 [5] Yu. M. Ivanov et al. Phys. Rev. Lett. 97 (2006) 144801; W. Scandale et al. Phys. Rev. Lett. 98 (2007) 154801.
 [6] M. V. Bondarenko. arXiv:0908.4503.
 [7] F. W. J. Olver. Asymptotics and Special Functions. Academic Press, New York, 1974.

[8] For such an orientation, all atomic planes of a diamond-type lattice, which silicon has, too, are equidistant, which makes all the inter-planar intervals identical.
 [9] Note that $\zeta^{(+)}$ is a symmetric function of $b+$ in the interval $d=2 < b < d=2-2$. That property in the following is extended to the deflection angle as a function of the impact parameter.
 [10] $\zeta^{(-)}$ is a symmetric function of $b-$ in the interval $d=2+2 < b < d=2$.
 [11] This cusp stems from vicinity of the symmetry point $b = \dots$, where $\left| \frac{d \nu_{v,r}}{d b} \right| \neq 0$ (see Fig. 5).